A Frequency-Reconfigurable Series-Fed Microstrip Patch Array With Interconnecting CRLH Transmission Lines

Muhammad Saeed Khan, Antonio-Daniele Capobianco, *Member, IEEE*, Adnan Iftikhar, Sajid Asif, *Student Member, IEEE*, Bilal Ijaz, *Member, IEEE*, and Benjamin D. Braaten, *Senior Member, IEEE*

***Abstract*—This letter presents the design of a frequency-reconfigurable series-fed microstrip patch array in which the elements are interconnected with composite right/left-handed transmission lines (CRLH-TLs). Reconfigurable CRLH-TLs are used instead of meandered microstrip lines to reduce the overall size of the array and provide two different zero-phase frequencies of operation for broadside radiation in both instances. p-i-n diodes were used to reconfigure the array by changing the electrical lengths of the patches and microstrip sections of the CRLH-TLs. The measurements were taken in an anechoic chamber to verify the simulation results. The array can be reconfigured to operate at 1.97 and 2.37 GHz.**

***Index Terms*—Composite right-/left handed transmission line, microstrip antenna array, series-fed array.**

I. Introduction

RAPID growth in the areas of WiMAX, WiFi, GPS, Bluetooth, and UWB [1] has led to the development of multiband platforms capable of accessing these wireless services. A major benefit of a reconfigurable antenna is the capability to access multiple services in a device without the need of multiple antennas, thus potentially saving space. In many of the reconfigurable antenna designs in published literature, p-i-n diodes, RF microelectromechanical system (MEMS) switches, and optical switches have been used to reconfigure the antennas [2]–[6]. Furthermore, microstrip patch antenna arrays are of great interest because of their small size, low cost, light weight, ease of manufacturing, and useful radiation patterns [7]. Typically, series-fed antenna arrays are driven from a single point and the radiating elements are connected in series by using conventional transmission lines of suitable length for the operating frequency. These transmission lines can be replaced by meandered lines and drive the elements of the array with the same voltage phase in order to achieve a broadside radiation pattern. However, at low microwave frequencies, meander lines can be very large. A possible way to overcome this size problem is to incorporate composite right/left-handed transmission lines (CRLH-TLs) into the feed network of a series-fed antenna array [8]–[13]. Efforts have been made previously to minimize the overall size of an array using CRLH-TLs [14]–[16]. However, these designs were limited to a single band of operation, and broadside radiation at two different frequencies may be difficult.

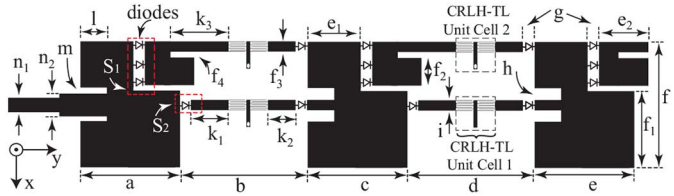

Fig. 1. Layout of the reconfigurable series-fed array with CRLH-TL interconnects. (a) Top view. (b) Bottom view. Dimensions are: $a = 43.2$ mm, $b = 39$ mm, $c = 43.7$ mm, $d = 39$ mm, $e = 44.4$ mm, $f = 49.5$ mm, $f_1 = 26.5$ mm, $f_2 = 15.3$ mm, $f_3 = 2.7$ mm, $f_4 = 2.5$ mm, $e_1 = 24.7$ mm, $e_2 = 24.5$ mm, $g = 1$ mm, $h = 2.65$ mm, $i = 2.7$ mm, $k_1 = 16.9$ mm, $k_2 = 8.2$ mm, $k_3 = 23.8$ mm, $l = 12.4$ mm, $m = 2$ mm, $n_1 = 3.65$ mm, and $n_2 = 4.86$ mm.

In this letter, the benefits of metamaterial-based transmission lines are combined with frequency reconfigurability to develop a compact series-fed microstrip patch array. The layout of the proposed array is shown in Fig. 1. It consists of three radiating patches and two nonradiating CRLH-TL interconnections between the radiating elements. The p-i-n diodes activate one of the CRLH-TLs at a time along with the particular sections of the main microstrip patch. These electrical switches reroute the current in a specific direction and alter the electrical lengths in the overall array, hence controlling the operating frequency of the array and achieving broadside radiation at two frequencies. Furthermore, this work is related to the single-frequency design reported in [16].

A. Design of the Array

The equivalent impedance model of a series-fed antenna array is shown in Fig. 2(a), which is classified as a standing

Manuscript received April 02, 2015; accepted May 24, 2015. Date of publication June 01, 2015; date of current version February 12, 2016.

M. S. Khan is with the Department of Electrical and Computer Engineering, North Dakota State University, Fargo, ND 58102 USA, and also with the Department of Information Engineering, Padova University, 35131 Padova, Italy.

A.-D. Capobianco is with the Department of Information Engineering, Padova University, 35131 Padova, Italy.

A. Iftikhar and S. Asif are with the Department of Electrical and Computer Engineering, North Dakota State University, Fargo, ND 58102 USA, and also with the Department of Electrical Engineering, COMSATS IIT, Islamabad 44000, Pakistan.

B. Ijaz is with the Department of Electrical Engineering, COMSATS IIT, Islamabad 44000, Pakistan.

B. D. Braaten is with the Department of Electrical and Computer Engineering, North Dakota State University, Fargo, ND 58102 USA (e-mail: benbraaten@ieee.org).

Color versions of one or more of the figures in this letter are available online at http://ieeexplore.ieee.org.

Digital Object Identifier 10.1109/LAWP.2015.2439637

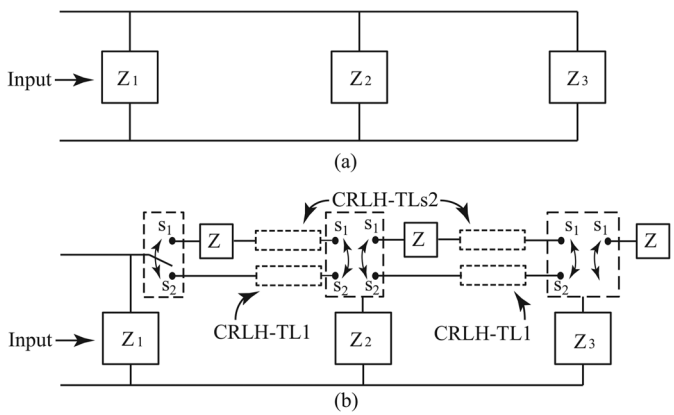

Fig. 2. (a) Circuit representation of a 3-element series-fed array with conventional microstrip interconnects and (b) circuit representation of a 3-element series-fed array with CRLH-TL interconnections showing the switching mechanism.

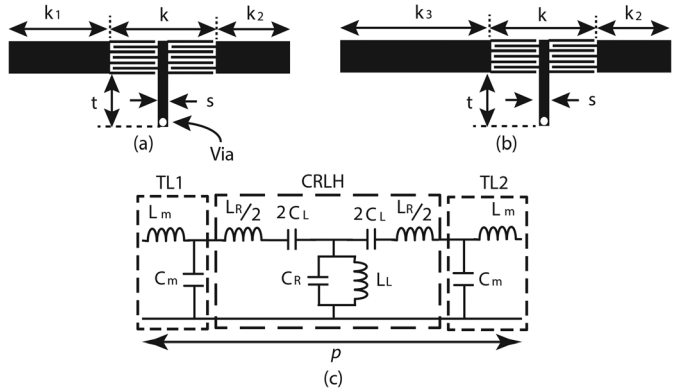

Fig. 3. (a) Layout of CRLH-TL unit cell 1. (b) Layout of CRLH-TL unit cell 2. (c) Circuit representation of CRLH-TL unit cells. Dimensions are: $k = 11.9$ mm, $k_1 = 16.9$ mm, $k_2 = 8.2$ mm, $k_3 = 23.8$ mm, $S = 1.3$ mm, $t = 7.26$ mm.

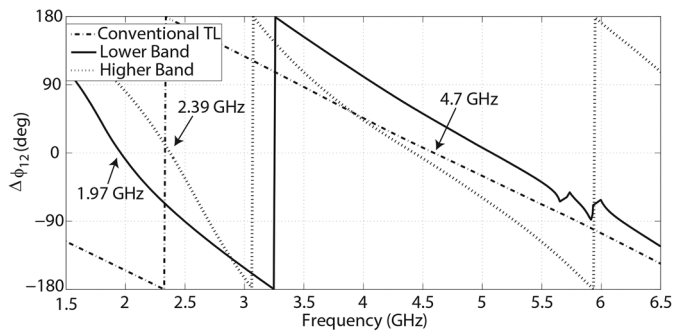

Fig. 4. Simulated S_{12} phase for the conventional transmission line with a total length of $k_1 + k + k_2$, higher band (unit cell 1) and lower band (unit cell 2).

wave array [17]. In these particular arrays, the feed is a single point, and Z_1, Z_2, and Z_3 represent the input impedance of each radiating element. The impedance of each antenna element and interconnecting transmission line has an important role in matching [18]. Furthermore, for a broadside radiation pattern, each element must be fed with the same voltage phase. This can be done by either designing the length of each interconnection to be a multiple of the TL wavelength or to introduce the CRLH-TLs that can be tuned to have a zero phase constant near the operating frequency [13] (i.e., a zero-phase frequency). To make the antenna array compact and reconfigurable, the switching mechanism shown in Fig. 2(b) was used. When the arm of the switch was connected to S_1, the CRLH-TL2 interconnects were activated. Then, when switch S_2 was connected to the arm, the CRLH-TL1 interconnects provided the path for current to travel along the array.

For a starting point, the CRLH-TL unit cells reported in [11] were adopted and finalized with a parametric study in HFSS. The layout and equivalent circuit of the CRLH-TL interconnects is shown in Fig. 3. It consists of series impedances (series-connected $C_{\rm L}$ and $L_{\rm R}$) as well as shunt impedances (parallel connected $L_{\rm L}$ and $C_{\rm R}$). $L_{\rm R}$ represents the parasitic inductance of the TL supporting wave propagation, and $C_{\rm R}$ represents the parasitic capacitance between the ground and the printed conductors on the top of the substrate. $C_{\rm L}$ represents the interdigitated capacitance between the fingers of the unit cell, and $L_{\rm L}$ is introduced due to the shunt stubs. When $L_{\rm L}$ and $C_{\rm L}$ are dominant for the frequencies of interest, a positive phase shift will be introduced by the CRLH-TL unit cell of length k. This phase shift can be changed to a particular frequency by adding a shunt per-unit-length capacitor, C_m, followed by a series per-unit-length inductor L_m on both sides on the CRLH-TL unit cell. With this configuration, the multiband CRLH-TL characteristics can be achieved. A Rogers RT/Duriod 5880 substrate with a thickness of 1.57 mm, $\varepsilon_{\rm r} = 2.2$, and the loss tangent of 0.0009 was chosen and used in the simulation environment with 0.5 oz copper.

The S_{12} phase of the unit cells at both operating frequencies is shown in Fig. 4. It can be seen that the zero-phase occurs at 2.39 GHz ($\lambda_2 = 126.5$ mm) when unit cell 1 [in Fig. 3(a)] was simulated. Then, when the length of the TL was increased, the zero-phase frequency was shifted to the lower band of 1.97 GHz ($\lambda_1 = 152.2$ mm), as shown in Fig. 4. For comparison, the phase introduced by a conventional 50-Ω microstrip interconnect is also plotted in Fig. 4. The length of this interconnect was chosen equal to the length of the CRLH-TL unit cell 1 in Fig. 3(a). It can be seen that the zero-phase frequency occurs at 4.7 GHz, which is almost double the zero-phase frequency of the CRLH-TL unit cell 1. Once the zero-phase configurations were determined, the CRLH interconnects were added to the array as shown in Fig. 1. Initially, the dimensions of the radiating patches were calculated using traditional half-wavelength antenna formulas, but later these dimensions were modified though a parametric study to optimize the results in HFSS. Furthermore, the overall length was chosen such that the spacing was approximately 0.5 lambda at the lower operating band and 0.67 lambda at the upper operating band. Finally, it should be mentioned that the zero-phase can be moved to other frequencies by changing the series inductance L_m of the CRLH-TL. In fact, to shift the zero-phase to a lower frequency, the length of the TL connecting with CRLH-TL is changed from k_1 to k_3, changing the series inductance L_m.

II. Simulated and Experimental Results

A. Prototype Testing

To demonstrate the functionality of the proposed frequency-reconfigurable series-fed array, a prototype was fabricated on the same Rogers RT/Duroid 5880 substrate as the simulations

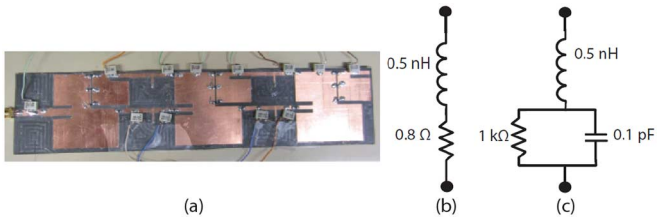

Fig. 5. (a) Photograph of the manufactured prototype. (b) Diode "ON" model and (c) diode "OFF" model.

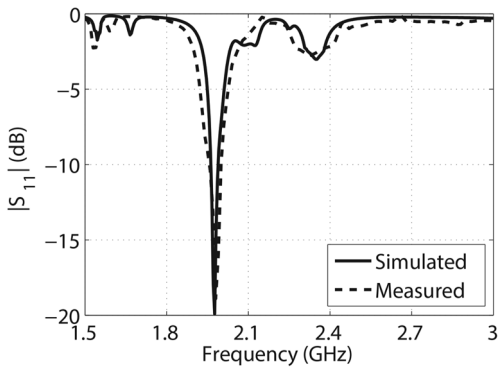

Fig. 6. Simulated and measured $|S_{11}|$ for the lower band with S_1 activated.

and is shown in Fig. 5(a). The CRLH-TL unit cells were connected to the array elements with switches consisting of surface-mount voltage-controlled p-i-n diodes. The control voltage ($+V = 0.7$ V) was applied to the conducting surface with RF chokes. The p-i-n diodes chosen were manufactured by Skyworks [19] (part number: SMP 1322), and to isolate the series-fed antenna array from the dc power source supplying the bias voltage, the RF chokes manufactured by Mini-circuits (part number: ADCH-80A) [20] were used.

The p-i-n diodes were modeled using the equivalent circuit defined in the data sheet, and the lumped elements were used in HFSS in a manner to the methods reported in [11] and [12]. For the ON state, the diodes were modeled using the equivalent circuit shown in Fig. 5(b), and for the OFF state, the diodes were modeled using the circuit in Fig. 5(c). Figs. 6 and 7 show the comparison of the S-parameters of the array with measurements. When switch S_2 was activated by biasing the lower diodes series and unbiasing the upper diode series, the antenna had a smaller electrical length and the current was passing through the CRLH-TL unit cell 1, hence resonating at the higher resonant frequency of 2.37 GHz (as shown in Fig. 7). When S_2 was turned "OFF" (i.e., when the lower diodes were unbiased) and S_1 was turned "ON" (i.e., upper diodes were biased), then a longer current path through the CRLH-TL unit cell 2 was introduced. This then resulted in the lower reconfigurable frequency of 1.97 GHz (as shown in Fig. 6). A fair comparison between simulated and measured results can be seen. Differences between the results in Figs. 6 and 7 could be due to: 1) the placement of the diodes during manufacturing; 2) the machine milling of the CRLH sections; 3) the nonideal RF chokes; and 4) the additional losses in the diodes (which is shown by the lower measured $|S_{11}|$ curves).

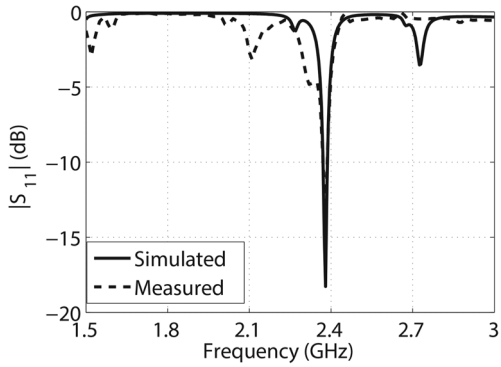

Fig. 7. Simulated and measured $|S_{11}|$ for the upper band with S_2 activated.

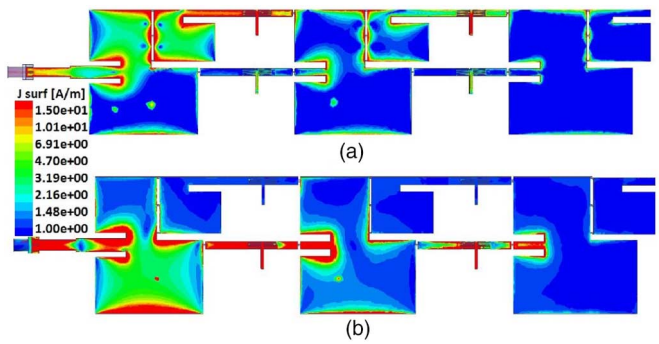

Fig. 8. Surface current distribution for (a) 1.97 and (b) 2.37 GHz.

B. Surface Current

The simulated surface current distribution at both operating frequencies is shown in Fig. 8. When the array is operating at the lower band, the current travels through the small patches to the CRLH-TL unit cell 2. There is a small induced current on CRLH-TL unit cell 1 as well, but it does not contribute to the lower resonant band due to its weak intensity. Similarly, when the array is operating at the upper band, the current flows through CRLH-TL unit cell 1 and there is much less current induced on the small patches and CRLH-TL unit cell 2.

C. Radiation Patterns, Gain, and Efficiency

Next, the normalized radiation pattern of the array was measured in both the lower and upper reconfigurable bands. In particular, the E_θ component in the yz-plane was measured at 1.97 and 2.37 GHz. The results from the measurements are shown in the Fig. 9, and a broadside radiation has been demonstrated at both switching frequencies.

Next, the gain of the proposed reconfigurable antenna array was measured in a fully calibrated anechoic chamber and compared to the simulated gain values from HFSS. When the array was configured for the lower band, the measured gain at the 1.97 GHz (resonant frequency) was 1.9 dBi while the simulated gain was 2.45 dBi. Also, while still configured for 1.97 GHz, the gain at 2.37 GHz (nonresonant frequency) was measured to be -6.0 dBi and simulated to be -5.2 dBi. This illustrated that the radiation from the antenna is in the desired lower reconfigurable band. Similarly, when the array was reconfigured for the upper operating band, the measured gain at 1.97 GHz (nonresonant frequency) was -5.5 dBi and the simulated gain

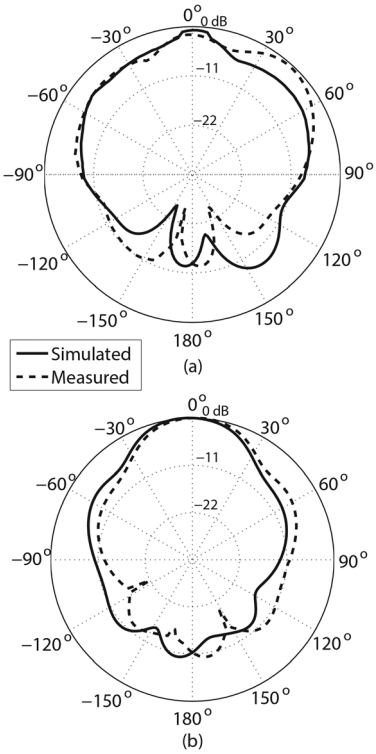

Fig. 9. Simulated and measured radiation pattern in the yz-plane for (a) 1.97 and (b) 2.37 GHz.

was −4.75 dBi. Then, the measured gain at 2.37 GHz (resonant frequency) was 3.5 dBi and the simulated gain was 3.95 dBi. Finally, the efficiencies of the proposed series-fed array were simulated in HFSS. The efficiency at 2.37 GHz was determined to be 0.785, and at 1.97 GHz, it was reduced to 0.47. This was due to the diodes used in switching at the lower band. Thus, one drawback of using RF p-i-n diodes on an antenna array is a reduction in efficiency. However, the array shows reasonable gain at both operating frequencies in the broadside direction, and efficiency can be improved using better diodes or MEMs switches.

III. Conclusion

In this letter, a new frequency-reconfigurable series-fed array based on zero-phase composite right/left-handed transmission lines (CRLH-TLs) was presented. Also, by the use of p-i-n diodes, the CRLH-TLs were activated and the current path was provided for the three interconnected microstrip patches. Simulated and measured results of the S-parameters and gain at both operating frequencies showed fair agreement. It was also observed that the zero-phase CRLH-TLs provided a reasonable broadside pattern at both of the reconfigurable frequencies.

References

[1] S. Yang, C. Zhang, H. K. Pan, A. E. Fathy, and V. K. Nair, "Frequency reconfigurable antenna for multiradio wireless platforms," *IEEE Microw. Mag.*, vol. 10, no. 1, pp. 66–83, Feb. 2009.

[2] C. W. Jung, M. Lee, G. P. Li, and F. De Flaviis, "Reconfigurable scan-beam single-arm spiral antenna integrated with RF-MEMS switches," *IEEE Trans. Antennas Propag.*, vol. 54, no. 2, pp. 455–463, Feb. 2006.

[3] D. E. Anagnostou *et al.*, "Design, fabircation, and measurements of an RF-MEMS-based self-similar reconfigurable antenna," *IEEE Trans. Antennas Propag.*, vol. 54, no. 2, pp. 422–432, Feb. 2006.

[4] S. Shelley, J. Costantine, C. G. Christodoulou, D. E. Anagnostou, and J. C. Lyke, "FPGA-controlled switch-reconfigured antenna," *IEEE Antennas Wireless Propag. Lett.*, vol. 9, pp. 355–358, 2010.

[5] C. J. Panagamuwa, A. Chauraya, and J. C. Vardaxoglou, "Frequency and beam reconfigurable antenna using photoconductive switches," *IEEE Trans. Antennas Propag.*, vol. 54, no. 2, pp. 449–454, Feb. 2006.

[6] Y. Tawk, A. R. Albrecht, S. Hemmady, G. Balakrishnan, and C. G. Christodoulou, "Optically pumped frequency reconfigurable antenna design," *IEEE Antennas Wireless Propag. Lett.*, vol. 9, pp. 280–283, 2010.

[7] M. M. Alam, M. M. R. Sonchoy, and M. O. Goni, "Design and performance analysis of microstrip array antenna," in *Proc. Prog. Electromagn. Res. Symp.*, Moscow, Russia, Aug. 18–21, 2009, pp. 1837–1842.

[8] A. Lai, T. Itoh, and C. Caloz, "Composite right/left-handed transmission line metamaterials," *IEEE Microw. Mag.*, vol. 5, no. 3, pp. 34–50, Sep. 2004.

[9] T. Jang *et al.*, "Switchable composite right/left handed (S-CRLH) transmission line using MEMS switches," *IEEE Microw. Wireless Compon. Lett.*, vol. 19, no. 12, pp. 804–806, Dec. 2009.

[10] G. Monti, R. De Paolis, and L. Tarricone, "Design of a 3-state reconfigurable CRLH transmission line based on MEMS switches," *Prog. Electromgn. Res.*, vol. 95, pp. 283–297, 2009.

[11] B. D. Braaten *et al.*, "A cascaded reconfigurable RH/CRLH-zero-phase microstrip transmission line unit cell," in *Proc. IEEE ICWITS*, Maui, HI, USA, Nov. 11–16, 2012, pp. 1–4.

[12] M.-I. Lai, T.-Y. Wu, J.-C. Hsieh, C.-H. Wang, and S.-K. Jeng, "Design of reconfigurable antennas based on an L-shaped slot and PIN diodes for compact wireless devices," *Microw., Antennas Propag.*, vol. 3, no. 1, pp. 47–54, 2009.

[13] M. Hashemi, N. Yuan, and T. Itoh, "Dual-band composite rigth left-handed matematerial concept," *IEEE Microw. Wireless compon. Lett.*, vol. 22, no. 5, pp. 248–250, May 2008.

[14] Z. Zhang and S. Xu, "A novel parellel-series feeding network of microstip patch arrays with composite right/left-handed transmission line for millimeter wave applications," *Int. J. Infrared Millim. Waves*, vol. 26, no. 9, pp. 1329–1341, Sep. 2005.

[15] M. A. Antoniades and G. V. Eleftheriades, "A metamaterial series-fed linear dipole array with reduced beam squinting," in *Proc. IEEE Int. Symp. Antennas Propag.*, Albuquerque, NM, USA, Jul. 2006, pp. 4125–4128.

[16] B. Ijaz *et al.*, "A series-fed microstrip patch array with interconnecting crlh transmission lines for WLAN applications," in *Proc. 7th EuCAP*, Gothenburg, Sweden, Apr. 12–18, 2013, pp. 2088–2091.

[17] T. Yuan, N. Yuan, and L. Li, "A novel series-fed taper antenna array design," *IEEE Antennas Wireless Propag. Lett.*, vol. 7, pp. 362–365, 2008.

[18] W. L. Stutzman and G. A. Thiele, *Antenna Theory and Design*, 2nd ed. New York, NY, USA: Wiley, 1998.

[19] Skyworks, Inc., "Skyworks, Inc.," [Online]. Available: http://www.skyworksinc.com

[20] Mini-Circuits, "Mini-Circuits," [Online]. Available: http://www.mini-circuits.com